



ELSEVIER

27 September 2001

Physics Letters B 517 (2001) 86–92

PHYSICS LETTERS B

www.elsevier.com/locate/npe

Matching parton showers to the QCD-improved parton model in deep-inelastic eP scattering

B. Pötter, T. Schörner

Max-Planck-Institut für Physik (Werner-Heisenberg-Institut), Föhringer Ring 6, 80805 Munich, Germany

Received 26 April 2001; received in revised form 16 July 2001; accepted 7 August 2001

Editor: P.V. Landshoff

Abstract

We have implemented a systematic procedure for combining parton shower algorithms with next-to-leading order QCD calculations for the case of jet production in deep-inelastic electron–proton scattering. Using this method we have computed inclusive jet cross sections and jet shapes for the case of single-jet production and compared them to the LEPTO generator and to data from the ZEUS Collaboration at HERA. We found good agreement between the data, LEPTO predictions and our calculations. © 2001 Elsevier Science B.V. Open access under [CC BY license](#).

1. Introduction

In the last two decades sophisticated event generators have been developed for all relevant physical scattering processes. For the case of eP scattering, generators like PYTHIA [1], HERWIG [2], LEPTO [3] or RAPGAP [4] are available. In the simplest case the event generation procedure falls into three steps. First, a one-parton final state is generated from the $\mathcal{O}(\alpha_s^0)$ quark-parton-model (QPM) matrix element. Next, a parton shower (PS) algorithm [2,5] is attached to the one-parton final state. The PS takes into account arbitrarily high orders in α_s , but only in the leading $\log Q^2$ approximation as opposed to the exact treatment in fixed order matrix elements. This implies that the region of small k_\perp around the original QPM quark is described quite well, which is important for the description of the internal properties of jets. Finally the PS is terminated at some lower cutoff Q_0^2 , where hadroniza-

tion models such as the Lund String model [6] can be used to simulate the transition of partons to hadrons.

The approximations involved in the construction of the PS allow to describe well only the region of small angle parton emission. The region of wide angle scattering should be more appropriately described by the hard QCD matrix elements of $\mathcal{O}(\alpha_s)$ which describe the QCD–Compton (QCDC) and boson–gluon fusion (BGF) processes with two final state partons. To include these processes into the event generators, the phase-space is separated into two complementary regions by means of some technical separation parameter, which we call R_{tech} in the following. In one (‘soft’) region, the QPM result plus PS is used to produce the cross section, whereas in the other (‘hard’) region the QCDC and BGF matrix elements are employed. The approximations involved in the PS approach suggest that the separation parameter R_{tech} should not be chosen too large in order to guarantee that wide angle scattering is appropriately described by the hard QCD matrix elements. One has to ensure that none of the partons generated by the

E-mail address: poetter@mppmu.mpg.de (B. Pötter).

PS populates the hard region above R_{tech} , since this would lead to double counting. Apart from separating the phase space into complementary regions, the parameter R_{tech} serves as a cutoff and ensures the finiteness of the QCD matrix elements, which are divergent in the region of soft and collinear particle emissions. A problem occurring at this stage is that the overall normalization of the cross section is not yet fixed. For the special case we are discussing here, the total cross section can be calculated beforehand, which can be used to normalize the contributions coming from the QPM and QCD matrix elements. A lower boundary for R_{tech} is obtained by the requirement that the sum of the QCDC and BGF contributions does not exceed the total cross section. Otherwise R_{tech} can be chosen freely.

The normalization of the individual contributions by calculating the total cross section beforehand is in general not feasible, e.g., for the case of dijet production in eP scattering. It is therefore desirable to find a general, systematic approach to fix the cross section when fixed order matrix elements are combined with PS algorithms. To reliably calculate the normalization of the cross section, the complete next-to-leading order (NLO) corrections to the leading order (LO) processes have to be calculated. This includes the calculation of the real soft and collinear regions, as well as of the virtual corrections. The NLO corrections to the QPM graph in deep-inelastic scattering (DIS) have long been evaluated [7]. Also for the DIS dijet case, several NLO calculations are available [8–11], which employ either the subtraction method [8,12,13] or the phase-space slicing technique [9,14–16] to treat the soft and collinear part of the real corrections. The problem of directly combining the NLO cross sections with the PS is the occurrence of large positive and negative weights in the NLO calculation which makes it practically difficult to obtain numerically stable results. Furthermore, it is not straightforward to use the hadronization models with negative weights.

Recently, several proposals were made to combine NLO QCD calculations, including the virtual corrections, with PS's [17–21]. In this Letter, we will rely on the method proposed by one of us (B.P.) in [20] and apply it to the case of single-jet inclusive cross sections in DIS eP scattering. The idea is to keep the separation of the phase-space into a soft and a hard region with

help of the R_{tech} parameter, but to use the full NLO calculation in the soft region instead of the LO one. To ensure that the weights generated in the soft region are always positive, a method adapted from [22] is employed where the s_{min} parameter of the phase-space slicing method is chosen such that the sum of the Born, virtual and soft and collinear contributions vanish. In this way, the NLO corrections are calculated from the hard matrix elements, integrated within the soft region down to the s_{min} cutoff, which will always yield positive weights. While in [22] the cutoff was adjusted by hand, in [20] it is calculated from the NLO corrections, thereby preserving the improved scale and scheme dependence of the NLO calculation.

The outline of the Letter is as follows. In Section 2 we specify how to generate events with positive NLO weights and how we have implemented the method for the case of single-jet production in DIS eP scattering. In Section 3 we calculate, for large Q^2 in the laboratory frame, inclusive jet cross sections and jet shapes and compare our calculations to measurements from the ZEUS Collaboration at HERA and to predictions from the LEPTO [3] event generator. We conclude with a short summary and an outlook.

2. Event generation with positive NLO weights

In eP scattering

$$e(k) + P(p) \rightarrow e(k') + X, \quad (1)$$

the simplest hadronic final state consists of a single jet with a large transverse energy E_T in the laboratory frame. The lowest order $\mathcal{O}(\alpha_s^0)$ partonic contribution to this single-jet cross section arises from the QPM subprocess. At NLO, the single-jet cross section receives contributions from the real and the one-loop virtual corrections. The real corrections consist of the BGF and QCDC processes which are divergent for collinear and soft emissions. These divergencies are cancelled by the virtual corrections or are absorbed into the parton density functions (PDFs) of the proton. To enable a numerical treatment of the real corrections, one can employ the phase-space slicing technique and introduce a parameter s_{min} which cuts out the singular regions. Within this method, the NLO cross section can be written as a sum of the one-parton final state up to $\mathcal{O}(\alpha_s)$ and the two-parton final state.

The one-parton final state reads

$$\begin{aligned} \sigma_{\text{had}}^{\text{1parton}}(s_{\text{min}}) &= \sigma_0 \sum_{i=q,\bar{q}} e_i^2 \int dx d\text{PS}^{(k'+1)} \\ &\times \left[f_i(x, \mu_F) (1 + \alpha_s(\mu_R) \mathcal{K}_{q \rightarrow q}(s_{\text{min}}, Q^2)) \right. \\ &\quad \left. + \alpha_s(\mu_R) C_i^{\overline{\text{MS}}}(x, \mu_F, s_{\text{min}}) \right] |M_{q \rightarrow q}|^2. \quad (2) \end{aligned}$$

The $f_i(x, \mu_F)$ are the proton PDFs, the Lorentz-invariant phase space measure $d\text{PS}^{(k'+n)}$ contains both the scattered electron and the partons from the photon-parton scattering process and the term σ_0 is defined as $\sigma_0 = 4(\pi\alpha)^2/(Q^4 x s)$. The e_i are the charges of the quarks. The factor $\mathcal{K}_{q \rightarrow q}$ which depends both on the phase-space slicing parameter s_{min} and on the hard scale of the process Q^2 contains the virtual and final state corrections and is specified in [20]. The function $C_i^{\overline{\text{MS}}}$ containing the initial state corrections is given by

$$\begin{aligned} C_i^{\overline{\text{MS}}}(x, \mu_F, s_{\text{min}}) &= \left(\frac{N_C}{2\pi} \right) \left[A_i(x, \mu_F) \ln\left(\frac{s_{\text{min}}}{\mu_F^2} \right) + B_i^{\overline{\text{MS}}}(x, \mu_F) \right]. \quad (3) \end{aligned}$$

The functions $A_i(x, \mu_F)$ and $B_i^{\overline{\text{MS}}}(x, \mu_F)$ are also specified in [20]. The final result, independent of s_{min} , is obtained by adding to the one-parton contribution the contribution containing the two-parton final state, integrated over those phase-space regions where any pair of partons i, j has $s_{ij} > s_{\text{min}}$ with $s_{ij} = (p_i + p_j)^2$:

$$\begin{aligned} \sigma_{\text{had}}^{\text{2parton}}(s_{\text{min}}) &= \sigma_0 \sum_{i=q,\bar{q}} e_i^2 \int_{|s_{ij}| > s_{\text{min}}} dx d\text{PS}^{(k'+2)} 4\pi\alpha_s(\mu_R) \\ &\times \left[f_i(x, \mu_F) |M_{q \rightarrow qg}|^2 \right. \\ &\quad \left. + \frac{1}{2} f_g(x, \mu_F) |M_{g \rightarrow q\bar{q}}|^2 \right]. \quad (4) \end{aligned}$$

The condition

$$\frac{d\sigma_{\text{had}}^{\text{1parton}}}{dx dQ^2}(s_{\text{min}}^{\text{nlo}}) = 0, \quad (5)$$

can be used to determine the function [20]

$$s_{\text{min}}^{\text{nlo}}(\mu_F, \mu_R, x, Q^2) = \exp\left[\eta - \sqrt{\eta^2 + \psi} \right], \quad (6)$$

in which

$$\eta = \ln(Q^2) - \frac{3}{4} + \frac{9}{16} \frac{A}{F}, \quad (7)$$

$$\begin{aligned} \psi &= -\ln^2(Q^2) + \frac{3}{2} \ln(Q^2) - \frac{\pi^2}{3} - \frac{1}{2} \\ &\quad + \frac{9}{8} \left[\frac{2\pi}{N_C \alpha_s} + \frac{B}{F} - \frac{A}{F} \ln(\mu_F^2) \right], \quad (8) \end{aligned}$$

and

$$F = \sum_{i=q,\bar{q}} e_i^2 f_i(x, \mu_F), \quad (9)$$

$$A = \sum_{i=q,\bar{q}} e_i^2 A_i(x, \mu_F), \quad (10)$$

$$B = \sum_{i=q,\bar{q}} e_i^2 B_i^{\overline{\text{MS}}}(x, \mu_F). \quad (11)$$

Inserting the $s_{\text{min}}^{\text{nlo}}$ function (6) into Eq. (4) as a lower integration boundary for each phase-space point (x, Q^2) will give the complete answer for the total cross section at NLO. It is important to note that the $s_{\text{min}}^{\text{nlo}}$ function depends on the factorization and renormalization scales, so that the improved scale dependence of the NLO cross section as opposed to the LO one is preserved. As was studied in detail in [20], the $s_{\text{min}}^{\text{nlo}}$ function Eq. (6) is small enough for the soft and collinear approximations to remain valid which are made to evaluate the $\mathcal{O}(\alpha_s)$ one-parton final states. The NLO single-jet cross section calculated within the standard approach could be reproduced within 1–2% with this method [20].

For the calculation of the cross sections in the next section, we have implemented the function $s_{\text{min}}^{\text{nlo}}$ into the DISENT program [8] and combined the NLO cross section thus obtained with the PS algorithm from PYHTIA [1]. The reason we chose DISENT is to be able to easily extend the results obtained here to the dijet case later on. In the dijet case also the subtraction terms from the subtraction method have to be used (see [20] for details). The steps we have performed to generate events are enumerated below. In the following the terms *one-jet* and *two-jet* describe only technical jet regions, which are not identical to the observed jets in the experiment. They are used to distinguish the soft (PS) region and the hard region.

(i) Define a one-jet (soft) region by $s_{ij} < R_{\text{tech}} Q^2$ for at least one pair of partons i, j . The partons are combined into a single jet.

(ii) The two-jet (hard) region is given by $s_{ij} > R_{\text{tech}} Q^2$ for all pairs of partons i, j . These partons are not recombined. The hard region is described by the two-parton matrix elements (BGF and QCDC). We do not attach the PS to the partons of the hard region, although this could in principle be done.

(iii) We want to describe the one-jet region with a PS algorithm and (positive) NLO weights. It is helpful to distinguish between the four-vectors of the event and the weight of the event. The weight inside the one-jet region is evaluated by calculating for each (x, Q^2) an $s_{\text{min}}^{\text{nlo}}$ according to Eq. (6), which provides the lower boundary in the integration of the QCD matrix elements. This ensures that the weights are positive for all phase-space points (x, Q^2) . The parton shower inside the one-jet region is obtained by redistributing the combined four-vector from step 1 with help of the PS algorithm from PYTHIA [1].

(iv) Reject any partons from the PS that lie outside the one-jet region to avoid double-counting.

After an event has been generated by this procedure, a jet algorithm has to be run which is the same as in the experiment. We point out that the soft and hard regions are distinguished by the parameter R_{tech} , not by $s_{\text{min}}^{\text{nlo}}$. The parameter R_{tech} should be larger than $s_{\text{min}}^{\text{nlo}}/Q^2$ but not too large to ensure that the hard region is appropriately described by the fixed order matrix elements. R_{tech} is typically of the order of 1. We have checked that our cross sections are not sensitive to the exact value of R_{tech} by varying it by a factor of 2. The starting scale for the PS is set by the matrix element cutoff [3].

We have not yet implemented the initial state PS, but only the final state PS. We have checked with LEPTO [3] that in the specific phase space region we are investigating in the next section, the effects of the initial state parton shower are below 5%, so that we can safely neglect these effects in this study. This holds for the inclusive spectra, as well as for the jet shapes. The parton emission due to the initial state PS populates mainly the forward region, which is excluded in the data with which we are comparing through kinematical cuts. The evolution of the incoming parton is taken into account through the evolution equations for the partons in the proton. Certainly, the initial state parton shower in general is important and we will include it in a future study. Furthermore, hadronization

effects have not been taken into account in our calculations. It is however feasible in our model to implement hadronization, since it can be naturally attached to the PS.

For all calculations in the next section we have set the renormalization and factorization scales equal to Q^2 and employed the CTEQ4M PDFs for the proton.

3. Results

The ZEUS Collaboration has measured inclusive jet cross sections in neutral current (NC) DIS eP scattering at $\sqrt{s} \simeq 300$ GeV in four regions of Q^2 , namely $Q^2 > 125, 500, 1000$ and 2000 GeV² [23,24]. The phase-space of the electron has been further reduced by restricting its energy $E_{e'}$ and the inelasticity y_e to $E_{e'} > 10$ GeV and $y_e < 0.95$, respectively. The jets were reconstructed using a k_T cluster algorithm [25] in the laboratory frame. The reconstructed jets were required to have a minimum transverse energy of $E_T > 14$ GeV and a pseudorapidity in the range $-1 < \eta < 2$.

Unfortunately we cannot show the ZEUS data, since they are still only preliminary. We have however checked that event generator LEPTO [3] reproduces very well the data, so that instead in Fig. 1 we can show a comparison of our calculation, given by the full line labeled ‘DISSET’, to the predictions from LEPTO in the four Q^2 regions mentioned above. We see an overall good agreement. Since our predictions are on parton level, we have checked the influence of the hadronization with LEPTO. We found that the overall effect of the hadronization is small, below 5%, with a tendency to lower the parton level predictions. We have furthermore checked that the PS changes the E_T distribution only marginally, also below 5%.

In [24] the data were compared to a standard NLO calculation with DISENT [8]. We have redone these calculations for comparison and also plotted the results in Fig. 1, shown as the dashed line labeled ‘standard DISENT’. Our results are in agreement with those from [24]. From this comparison we deduce that our calculation reproduces correctly the standard NLO result, which confirms the findings in [20].

We emphasize that the correct normalization of the cross sections is a non-trivial result of our procedure. We obtained the normalization without using informa-

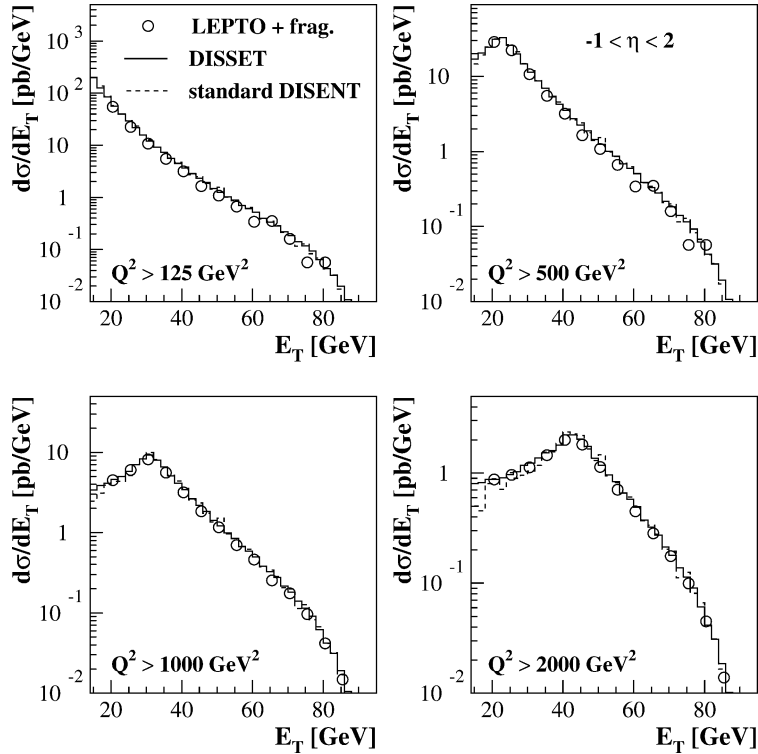


Fig. 1. Differential cross sections $d\sigma/dE_T$ for inclusive jet production in NC DIS events integrated over $-1 < \eta < 2$ for $Q^2 > 125, 500, 1000$ and 2000 GeV^2 . Our calculation labeled 'DISSET' (full line) is compared to an NLO calculation, labeled 'standard DISENT' (dashed line) and to predictions derived using the LEPTO generator (open circles).

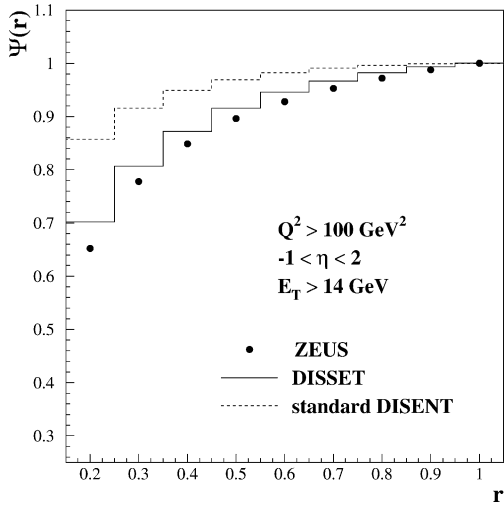


Fig. 2. Integrated jet shape $\Psi(r)$ in NC DIS events integrated over $Q^2 > 100 \text{ GeV}^2$ for jets with $E_T > 14 \text{ GeV}$ and $-1 < \eta < 2$. The ZEUS data are compared to our calculation (full line) and to a NLO calculation (dashed line).

tion from the total eP scattering cross section. The normalization comes directly from the NLO matrix elements, modified by the g_{\min}^{nlo} function.

We proceed to a comparison of our calculation with jet shape measurements. The ZEUS Collaboration has measured the differential and integrated shape of jets in neutral current DIS events with $Q^2 > 100 \text{ GeV}^2$ for jets with E_T above 14 GeV and $-1 < \eta < 2$ [26]. The jets are reconstructed using an iterative cone algorithm in the (η, ϕ) plane [27,28]. For the scattered electron further restrictions are $E_{e'} > 10 \text{ GeV}$ and $y_e < 0.95$, as for the previously discussed data. The differential jet shape is defined as the average fraction of the jet's transverse energy that lies inside an annulus in the (η, ϕ) plane of inner (outer) radius $r - \Delta r/2$ ($r + \Delta r/2$) concentric with the jet defining cone [29]:

$$\rho(r) = \frac{1}{N_{\text{jets}}} \frac{1}{\Delta r} \sum_{\text{jets}} \frac{E_T(r - \Delta r/2, r + \Delta r/2)}{E_T(0, R)}. \quad (12)$$

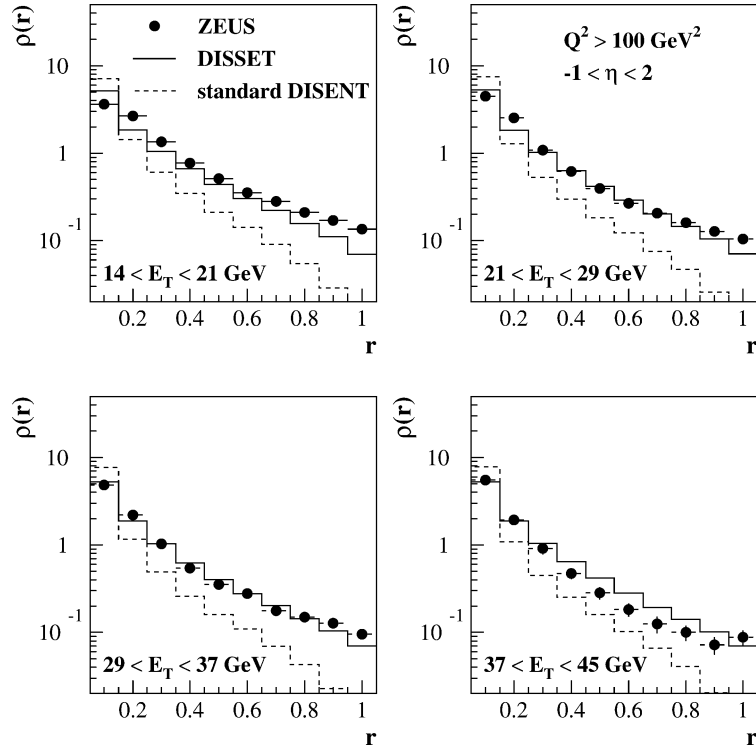


Fig. 3. Integrated jet shape $\rho(r)$ in NC DIS events integrated over $Q^2 > 100 \text{ GeV}^2$ for jets with $-1 < \eta < 2$ in four different ranges of E_T . The ZEUS data are compared to our calculation (full line) and to a NLO calculation (dashed line).

Here, $E_T(r - \Delta r/2, r + \Delta r/2)$ is the transverse energy within the given annulus and N_{jets} is the total number of jets in the sample. The differential jet shape has been measured for r values varying from 0.05 to 0.95 in $\Delta r = 0.1$ increments. The integrated jet shape is defined by

$$\Psi(r) = \frac{1}{N_{\text{jets}}} \sum_{\text{jets}} \frac{E_T(0, r)}{E_T(0, R)}. \quad (13)$$

By definition, $\Psi(R) = 1$. It has been measured for r values varying from 0.1 to 1.0 also in increments of $\Delta r = 0.1$.

In Fig. 2 we compare our calculation (full line) and a standard NLO calculation (dashed line) to the ZEUS data which are corrected to hadron level. The description of the jet shape within our approach is rather good. The jets produced are slightly too narrow, our calculation being about 8% above the data in the lowest r bin. We have checked with LEPTO that the hadronization effects can account

for the difference between data and prediction, i.e., including hadronization in our calculation would bring our results to good agreement with the data. We furthermore see that the standard NLO prediction is much too large for all r . This implies that the jets produced by the standard calculation are not broad enough. Reducing the cross sections by taking into account hadronization is not sufficient for the standard NLO calculation. This result is not surprising since the standard NLO calculation provides only a LO prediction for the jet shape in which at maximum two partons are combined to give a jet.

In Fig. 3 we finally compare our calculations to the ZEUS differential jet shapes for four different E_T regions. We find similar results as for the integrated jet shapes. The standard NLO calculation (dashed line) is clearly too narrow in all four E_T regions, whereas our calculation (full line) gives a much better description. In the lowest E_T bin our calculation produces slightly too narrow jets, whereas in the largest E_T bin the jets

tend to be too broad. Using LEPTO, we have checked the hadronization corrections also for the differential jet shapes and found the discrepancies between our calculation on the parton level and the data can be accounted for by hadronization effects.

4. Summary and outlook

We have investigated the method described in [20] to combine a fixed NLO QCD calculation, including the real soft and collinear as well as the virtual corrections, with a leading log PS. We have implemented the method in DISENT and attached the PS from PYTHIA. We have compared our calculation with data from ZEUS for jet shape measurements in the laboratory frame and with predictions from the LEPTO program for inclusive jet spectra. For both comparisons, good agreement with our model was found. In addition, good agreement was found between the standard NLO calculation and our results for the case of the inclusive spectra in transverse energy, where the influence of the PS is marginal. This shows that we have obtained the correct NLO normalization of the cross sections together with a good description of the internal structure of the jets.

To obtain a full event generator, the initial state PS as well as hadronization need to be implemented in our program package. This will be done in the near future. The next, more complicated step is to proceed to the two-jet final states and combine the NLO calculations for this case with the PS. Although some details have to be clarified for this case, we could show the principle feasibility of our method.

References

- [1] T. Sjöstrand, *Comput. Phys. Commun.* 82 (1994) 74.
- [2] G. Marchesini et al., *Comput. Phys. Commun.* 67 (1992) 465.
- [3] G. Ingelman, A. Edin, J. Rathsman, *Comput. Phys. Commun.* 101 (1997) 108.
- [4] H. Jung, *Comput. Phys. Commun.* 86 (1995) 147.
- [5] M. Bengtsson, T. Sjöstrand, *Z. Phys. C* 37 (1988) 465; M. Bengtsson, G. Ingelman, T. Sjöstrand, in: R.D. Peccei (Ed.), *Proceedings of the HERA Workshop 1987*, Vol. 1, DESY, Hamburg, 1988, p. 149.
- [6] B. Andersson, G. Gustafson, G. Ingelman, T. Sjöstrand, *Phys. Rep.* 97 (1983) 31.
- [7] G. Altarelli, R.K. Ellis, G. Martinelli, *Nucl. Phys. B* 143 (1978) 521; G. Altarelli, R.K. Ellis, G. Martinelli, *Nucl. Phys. B* 146 (1978) 544, Erratum; G. Altarelli, R.K. Ellis, G. Martinelli, *Nucl. Phys. B* 157 (1979) 461; A. Mendez, *Nucl. Phys. B* 145 (1978) 199; A. Mendez, T. Weiler, *Phys. Lett. B* 83 (1979) 221; R.D. Peccei, R. Rückl, *Nucl. Phys. B* 162 (1980) 125; Ch. Rumpf, G. Kramer, J. Willrodt, *Z. Phys. C* 7 (1981) 337.
- [8] S. Catani, M.H. Seymour, *Phys. Lett. B* 378 (1996) 287; S. Catani, M.H. Seymour, *Nucl. Phys. B* 485 (1997) 291.
- [9] D. Graudenz, *Phys. Rev. D* 19 (1994) 3291; D. Graudenz, *Phys. Lett. B* 256 (1992) 518.
- [10] E. Mirkes, D. Zeppenfeld, *Phys. Lett. B* 380 (1996) 23; E. Mirkes, D. Zeppenfeld, *Acta Phys. Pol. B* 27 (1996) 1392.
- [11] G. Kramer, B. Pötter, *Eur. Phys. J. C* 5 (1998) 665; B. Pötter, *Eur. Phys. J. C* 5 (1999) 1.
- [12] R.K. Ellis, D.A. Ross, A.E. Terrano, *Nucl. Phys. B* 178 (1981) 421.
- [13] Z. Kunszt, D.E. Soper, *Phys. Rev. D* 46 (1992) 196.
- [14] K. Fabricius, G. Kramer, G. Schierholz, I. Schmitt, *Z. Phys. C* 11 (1982) 315; F. Gutbrod, G. Kramer, G. Rudolph, G. Schierholz, *Z. Phys. C* 35 (1987) 543.
- [15] H. Baer, J. Ohnemus, J.F. Owens, *Phys. Rev. D* 40 (1989) 2844; H. Baer, J. Ohnemus, J.F. Owens, *Phys. Rev. D* 42 (1990) 61; H. Baer, J. Ohnemus, J.F. Owens, *Phys. Lett. B* 234 (1990) 127.
- [16] W.T. Giele, E.W.N. Glover, *Phys. Rev. D* 46 (1992) 1980.
- [17] C. Friberg, T. Sjöstrand, in: A.T. Doyle, G. Grindhammer, G. Ingelman, H. Jung (Eds.), *Proceedings of the DESY Workshop on Monte Carlo Generators for HERA Physics*, DESY, Hamburg, 1999, hep-ph/9906316.
- [18] J. Collins, *JHEP* 0005 (2000) 4.
- [19] S. Mrenna, preprint UCD-99-4, hep-ph/9902471.
- [20] B. Pötter, *Phys. Rev. D* 63 (2001) 114017.
- [21] M. Dobbs, *Phys. Rev. D* 64 (2001) 034016.
- [22] H. Baer, M.H. Reno, *Phys. Rev. D* 44 (1991) R3375; H. Baer, M.H. Reno, *Phys. Rev. D* 45 (1992) 1503; H. Baer, M.H. Reno, *Phys. Rev. D* 54 (1996) 2017.
- [23] M. Przybycien (for the ZEUS Collaboration), *Nucl. Phys. B Proc. Suppl.* 79 (1999) 481.
- [24] ZEUS Collaboration, J. Breitweg et al., *Europhysics Conference on High Energy Physics 99*, Tampere, Finland, July, 1999, contributed paper.
- [25] S.D. Ellis, D.E. Soper, *Phys. Rev. D* 48 (1993) 3160.
- [26] ZEUS Collaboration, J. Breitweg et al., *Eur. Phys. J. C* 8 (1999) 367.
- [27] CDF Collaboration, F. Abe et al., *Phys. Rev. D* 45 (1992) 1448.
- [28] J. Huth et al., in: E.L. Berger (Ed.), *Proceedings of the 1990 DPF Summer Study on High Energy Physics*, Snowmass, Colorado, World Scientific, Singapore, 1992, p. 134.
- [29] S.D. Ellis, Z. Kunszt, D.E. Soper, *Phys. Rev. Lett.* 69 (1992) 3615.